Sulfur Poisoning and Regeneration of NO_x Storage−Reduction $Cu/K_2Ti_2O_5$ Catalyst

Qiang Wang,*,† Jiahua Zhu,‡ Suying Wei,§ Jong Shik Chung,†,|| and Zhanhu Guo*,‡

School of Environmental Science and Engineering and Department of Chemical Engineering, POSTECH, Pohang 790-784, Republic of Korea, and Integrated Composites Laboratory (ICL), Dan F. Smith Department of Chemical Engineering, and Department of Chemistry and Physics, Lamar University, Beaumont, Texas 77710

A new $Cu/K_2Ti_2O_5$ catalyst has been developed recently to remove NO_x through the NO_x storage−reduction (NSR) process. However, its NSR performance in the presence of sulfur has not been investigated. In this article, the sulfur poisoning of the NO_x storage−reduction catalyst $Cu/K_2Ti_2O_5$ and the corresponding deactivation mechanisms are reported for the first time. The effect of the sulfur concentration, adsorption/regeneration cycling tests, and temperature-programmed regeneration are studied. At low temperatures, the poisoning effect is negligible when the SO_2 concentration is lower than 20 ppm, and the sulfated samples can be easily regenerated by 3.5% H_2 at 550 °C. However, at high temperatures, the sulfur species are adsorbed on K^+ sites to form K_2SO_4 and, consequently, induce a structure transformation from $K_2Ti_2O_5$ to $K_2Ti_6O_{13}$ nanoparticles. The structural change is reversible, and the sulfated catalyst can be regenerated by hydrogen at 650−700 °C.

1. Introduction

NO_x storage and reduction (NSR) catalysts have been developed and well-established as a promising technology for the reduction of NO_x under lean operating conditions. They store NO_x as nitrates (or nitrite) under lean conditions and allow nitrate (or nitrite) decomposition and NO_x reduction during short rich conditions.[1−4] Typical NSR catalysts consist of precious metals (e.g., Pt, Rh), alkali/alkaline metal oxides (e.g., Ba, K, Mg, and Ca) as the NO_x storage materials, and metal oxides (e.g., γ-Al_2O_3, TiO_2−ZrO_2) as the support.[5−8] However, for a broad market penetration of NSR catalysts, significant technological improvements are necessary, especially in terms of catalyst durability caused by thermal aging and sulfur poisoning.[9,10]

Currently, commercial diesel fuels typically contain about 350 ppm of sulfur. The 2007 on-road diesel emission standards allow a maximum value of 15 ppm sulfur content in diesel fuel, and this ultra-low-sulfur fuel is expected to contribute less than 1 ppm to the total sulfur content of the exhaust gas.[9] In typical lean exhaust, sulfur is present mainly in the form of SO_2, as most of the sulfur compounds become oxidized during combustion. In other words, SO_2 represents the major source of sulfur poisoning of NSR catalysts. Sulfur poisoning during lean operation is similar to NO_x storage, in which sulfates are formed from SO_2 in the engine exhaust and stored in conjunction with the alkali or alkaline-earth metals.[11,12] The sulfur can also poison the precious metals and the supports.[13,14] As sulfates are thermodynamically more stable than nitrates, sulfur accumulates over time and blocks the formation of nitrates.

For practical applications, periodic removal of the deposited sulfur from NSR catalysts is highly necessary.[15,16] If the desulfurization is effective, NSR performance could be increased to its original or at least an acceptable level by releasing sulfur from the Pt and trapping sites. However, the decomposition temperature of $BaSO_4$ is much higher than that of $Ba(NO_3)_2$.[17] Although the decomposition temperature could be highly reduced to a much lower level (∼650 °C) in a reducing environmental, it is still not low enough to prevent the thermal degradation of alkali-doped-type NSR catalysts. Therefore, the current trend for conventional NSR catalysts is trying to achieve an efficient and low-impact desulfurization, without inducing extensive thermal degradation.[18,19]The regeneration process of the storage component also depends on time and the nature of the reductant.[10] Until now, it has been widely accepted that hydrogen is more reductive than carbon monoxide and hydrocarbons.[4,20]

In addition to the effort to modify the regeneration strategy, decreasing the stability of adsorbed sulfur species or synthesizing a more thermally stable NSR catalyst is an alternative approach to overcome the sulfur poisoning problem. Recently, we have developed a series of $K_2Ti_2O_5$-based NSR catalysts that adsorb NO_x over a very wide temperature range (200−600 °C).[21,22] Mechanistic investigations indicate that, at low temperature, NO_x is adsorbed on oxygen vacancies, and the thermal stability of such adsorbed NO_x species is much lower than the stabilities on alkali metals. In the same way, we expect that the thermal stability of sulfur species adsorbed on oxygen vacancies could be much lower than that of the sulfates (e.g., $BaSO_4$, or K_2SO_4). Even more, thermal stability tests have shown that $Pt/K_2Ti_2O_5$ is highly stable after pretreatment at 700 °C for 200 h.[22] This provides the possibility of regenerating the sulfated samples at high temperature (700 °C), without leading to any decrease of NO_x storage capacity.

Our previous studies have revealed that $Cu/K_2Ti_2O_5$ has two NO_x adsorption temperature ranges.[21] In the low-temperature range (200−400 °C), the NO_x adsorption rate is very high, and saturation is reached after about 30 min; the oxygen vacancies formed on the $K_2Ti_2O_5$ support during lean period are the adsorption sites. In contrast, in the high-temperature range (500−600 °C), although the adsorption rate is relatively low, a huge amount of NO_x adsorption (1.2 mmol/g) is achieved; in this case, a structure switching between $K_2Ti_2O_5$ and $K_2Ti_6O_{13}$ is proposed to explain the high-temperature NO_x storage and reduction on $Cu/K_2Ti_2O_5$.[21] Because of its superior thermal

* To whom correspondence should be addressed. E-mail: wang_qiang@ices.a-star.edu.sg (Q.W.), zhanhu.guo@lamar.edu (Z.G.).
† School of Environmental Science and Engineering, POSTECH.
‡ Integrated Composites Laboratory (ICL), Dan F. Smith Department of Chemical Engineering.
§ Department of Chemistry and Physics, Lamar University.
|| Department of Chemical Engineering, POSTECH.

10.1021/ie1009525
Published on Web 07/09/2010

stability, $Cu/K_2Ti_2O_5$ has proved to be a promising high-temperature NSR catalyst, as well as a potential low-temperature NSR catalyst once the reduction activity is increased. However, all of those tests were carried out without the presence of SO_2. Because SO_2 might compete with NO_x for the adsorption sites, its influence on the performance of this novel NSR catalyst ($Cu/K_2Ti_2O_5$) is of great importance for its practical usage. Sulfur poisoning is one of the most important issues that should be investigated.

In the present work, both the low- and high-temperature sulfur poisoning effects of the NO_x storage−reduction catalyst $Cu/K_2Ti_2O_5$ were investigated using various analytical means. During sulfur adsorption and desorption, the corresponding morphological changes and mechanisms were studied using X-ray diffraction (XRD), Fourier transform infrared (FTIR) spectroscopy, X-ray photoelectron spectroscopy (XPS), and scanning electron microscopy (SEM). The influence of the SO_2 concentration and doping metals, the H_2 regeneration performance, and the NO_x/SO_2 competition during adsorption were also investigated and are reported here.

2. Experimental Section

2.1. Synthesis of Catalysts. $K_2Ti_2O_5$ and $K_2Ti_6O_{13}$ were synthesized by a solid-state reaction method.[23−25] Briefly, a specified amount (6.91 g for $K_2Ti_2O_5$ or 2.30 g for $K_2Ti_6O_{13}$) of K_2CO_3 (Yakuri Pure Chemical Co., Ltd.) was mixed with 7.99 g of TiO_2 (Hombikat UV 100) by ball milling for 24 h, followed by calcination at 850 or 1180 °C (for $K_2Ti_2O_5$ or $K_2Ti_6O_{13}$, respectively) for 10 h in air to obtain $K_2Ti_2O_5$ and $K_2Ti_6O_{13}$.

In addition, 7.5 wt % $Cu/K_2Ti_2O_5$, 2 wt % $Pt/K_2Ti_2O_5$, and 2 wt % $Ce/K_2Ti_2O_5$ were prepared by incipient-wetness impregnation with $Cu(NO_3)_2 \cdot 3H_2O$ (Shinyo pure chemicals Co., Ltd.), $H_2PtCl_6 \cdot 5.7H_2O$ (Kojima Chemicals Co., Ltd.), and $Ce(NO_3)_3 \cdot 6H_2O$ (Aldrich Co., Ltd.) as precursors on the $K_2Ti_2O_5$ support. Finally, 7.5 wt % Cu−5 wt % $Co/K_2Ti_2O_5$ was synthesized by successively impregnating $Co(NO_3)_2 \cdot 6H_2O$ (Junsei Chemical Co., Ltd.) and $Cu(NO_3)_2 \cdot 3H_2O$ on $K_2Ti_2O_5$. All of the as-prepared samples were dried in an oven overnight and further calcined at 850 °C for 10 h.

2.2. Characterization of Catalysts. XRD patterns were obtained by using an X-ray analyzer (XRD, M18XHF, Mac Science Co., Ltd., Yokohama, Japan). Ni-filtered Cu Kα radiation ($\lambda = 1.5415$ Å) was used with an X-ray gun operated at 40 kV and 200 mA. Diffraction patterns were obtained within the range of $2\theta = 5-70°$ with a step size of 0.02°. The morphologies of the catalysts were investigated by field-emission scanning electron microscopy (FE-SEM; Hitachi, S-4200), and the chemical compositions were determined by energy-dispersive X-ray (EDX) analysis. FTIR experiments were performed using a Perkin-Elmer 2000 FTIR spectrophotometer. A self-supporting thin disk 13 mm in diameter was prepared by pressing 1 mg of catalyst powder and 14 mg of KBr (FTIR-grade, Aldrich Chem. Co.) using a manual hydraulic press. All spectra were measured with 4 cm^{-1} resolution. XPS analysis was performed with a VG Scientific ESCALAB 220-IXL instrument using nonmonochromated Mg Kα radiation (1253.6 eV). The binding energy was corrected using a reference of the contaminated carbon (284.6 eV). Sulfur content was analyzed with a LECO SC-432 sulfur analyzer. The quantitative estimation of sulfur is based on high-temperature combustion (1370 °C), where all sulfur-containing compounds were oxidized to SO_2 and SO_3. SO_3 was subsequently reduced to SO_2, and the total amount of SO_2 was analyzed in an IR cell.

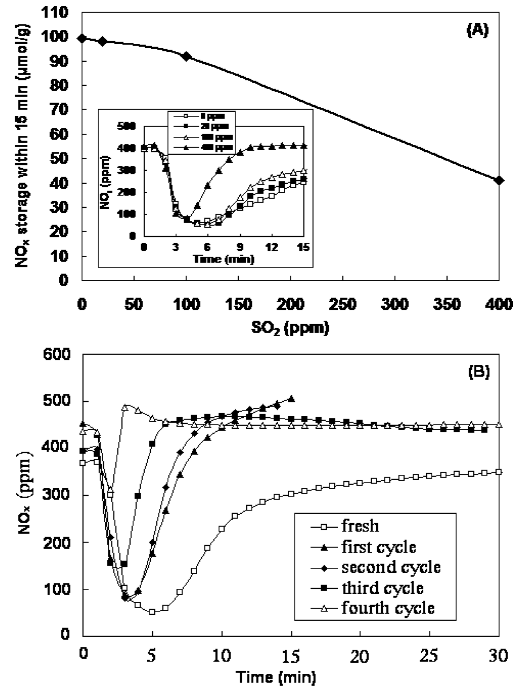

Figure 1. (A) Effect of SO_2 poisoning on NO_x adsorption at 400 °C (0.3 g of catalyst). Feed: 400 ppm NO, 0−400 ppm SO_2, 5% O_2 with He balance, 200 mL/min. (B) Repeated storage of NO_x in the presence of SO_2 over reduced $Cu/K_2Ti_2O_5$ at 400 °C (0.3 g of catalyst). NO_x storage: 400 ppm NO, 400 ppm SO_2, and 5% O_2 with He balance, 200 mL/min. Reduction: 3.5% H_2 with He balance at 400 °C for 30 min, 200 mL/min.

2.3. Activity Tests. Catalytic tests were carried out in a quartz flow reactor (10-mm internal diameter) with a fixed bed. The reactor was heated by an electric furnace controlled by a proportional−integral−derivative (PID) temperature controller (Han Kook Electronic Co.), and the temperature of the catalyst was measured by using a K-type thermocouple (outer diameter of 0.5 mm) that was immersed in the catalyst bed. The feed and product compositions were monitored by an online quadrupole mass spectrometer (Balzers Pfeiffer) and a NO_x analyzer (Chemiluminescence NO−NO_2−NO_x analyzer, model 42C, high-level, Thermo Environmental Instruments).

The influence of SO_2 on NO_x storage in the low-temperature range was evaluated by isothermal NO_x storage at 400 °C. Typically, 0.3 g of catalyst was used for each run, and the inlet gases contained 400 ppm NO, 5% O_2, a certain amount of SO_2 (0−400 ppm), and He as the carrier gas.

The sulfur poisoning effect at high temperature was evaluated by lean−rich cycling tests at 550 °C with typically 0.6 g of $Cu/K_2Ti_2O_5$. The lean phase contained 400 ppm NO and 5% O_2 in helium carrier, and the rich phase contained 400 ppm NO and 3.5% H_2 in helium carrier. The total gas flow during the lean−rich cycling experiment was maintained constant at 200 mL/min. To evaluate the sulfur effect, a certain amount of SO_2 was also added to both the lean and rich phases in some cases. The stability of deposited sulfur was evaluated by temperature-programmed reduction (TPR) with 3.5% H_2 from room temperature to 750 °C.

3. Results and Discussion

3.1. Sulfur Poisoning at Low Temperature. The sulfur poisoning effect on the NO_x storage capacity of $Cu/K_2Ti_2O_5$ was first studied in the presence of various amounts of SO_2 (0−400 ppm) (Figure 1A). The NO_x storage capacity was calculated based on the difference between the inlet and outlet

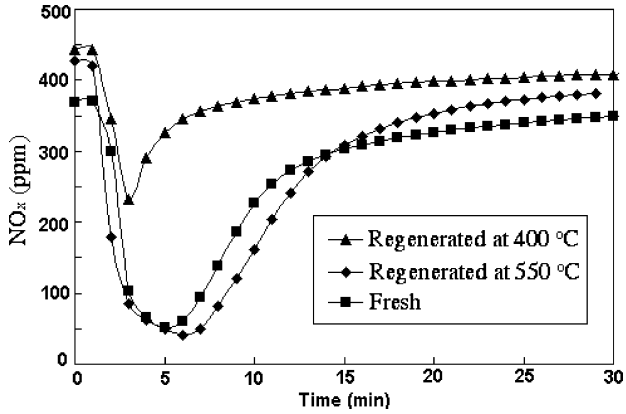

Figure 2. Effect of regeneration temperature on the NO_x storage of sulfur-poisoned $Cu/K_2Ti_2O_5$ (0.3 g of catalyst). Regeneration conditions: 3.5% H_2 with He balance at 400 or 550 °C for 30 min, 200 mL/min. NO_x storage: 400 ppm NO, 5% O_2 with He balance at 400 °C, 200 mL/min.

NO_x contents within 15 min. When the SO_2 concentration was less than 20 ppm, the sulfur poisoning effect was not significant, and only a slight decrease in NO_x storage amount was observed. The NO_x adsorption capacity gradually decreased with increasing SO_2 concentration, indicating that SO_2 molecules compete with NO_x molecules for the adsorption sites. When the SO_2 concentration reached 400 ppm, only 40% of the original NO_x adsorption capacity was achieved.

The SO_2 poisoning effect was further investigated during a repeated adsorption/regeneration cycling test with 400 ppm NO_2 and 400 ppm SO_2. The test was carried out as follows: After each adsorption, the sample was regenerated with 3.5% H_2 at 400 °C for 30 min; then the adsorption/regeneration cycle was repeated four more times. Figure 1B shows the outlet NO_x concentration as a function of time during the adsorption process. The NO_x adsorption capacity gradually decreased with increasing number of adsorption/regeneration cycles. After four cycles, the catalyst was observed to lose 98% of its NO_x storage capacity, indicating that the adsorbed SO_2 species could not be released at 400 °C. After four cycles, all adsorption sites were occupied by SO_2, leading to a complete loss of NO_x adsorption.

Figure 2 shows the regeneration of sulfated NSR catalyst at a higher temperature (550 °C). Fortunately, the capacity can be completely regenerated at 550 °C using 3.5% H_2. It is well-known that typical NO_x storage materials (e.g., $Pt-Ba/Al_2O_3$) have a poor resistance to SO_2 because it gradually forms $BaSO_4$.[26] In contrast, for $Cu/K_2Ti_2O_5$, the low-temperature adsorption sites are oxygen vacancies, not alkali/alkaline metal oxides, and the thermal stability of adsorbed SO_x species on oxygen vacancies is much lower than that of the sulfates (e.g., $BaSO_4$, K_2SO_4, etc.). This explains that the low-temperature sulfated $Cu/K_2Ti_2O_5$ can be easily regenerated at a much lower temperature (550 °C).

The present study demonstrates that the NO_x storage capacity of $Cu/K_2Ti_2O_5$ is barely affected by SO_2 if its concentration is below 20 ppm. For real diesel engines operating at steady conditions, the temperature of the emission gas under fuel-lean conditions is usually 400 °C; however, it increases to 550 °C under fuel-rich conditions. This high temperature will be ideal to regenerate the sulfated $Cu/K_2Ti_2O_5$, which might occur with an accidental input of high-content sulfur.[12]

3.2. Sulfur Poisoning at High Temperature. 3.2.1. Effect of the Doping Metals. Recently, Cu has also received much attention because of its capability to simultaneously remove SO_2 and NO_x from flue gas.[27−31] Cu readily adsorbs SO_2 in the presence of O_2 to form $CuSO_4$ at low temperature (200−400 °C), and the formed $CuSO_4$ is relatively easy to regenerate under reducing conditions. In addition, copper compounds (Cu, CuO, and $CuSO_4$) are active in the selective catalytic reduction (SCR) of NO_x to N_2.[27−31] In this section, the sulfur deposition on $Cu/K_2Ti_2O_5$ is compared with those on $Cu-Co/K_2Ti_2O_5$, $Pt/K_2Ti_2O_5$, and $Ce/K_2Ti_2O_5$ by pretreating these catalysts with a lean−rich cycling test (lean 5 min and rich 2 min) at 550 °C with 50 ppm SO_2. Figure 3 shows that $Cu/K_2Ti_2O_5$ accumulates the least amount of sulfur. Among these catalysts, the tendency to accumulate sulfur follows the order $Ce/K_2Ti_2O_5 > Cu-Co/K_2Ti_2O_5 > Pt/K_2Ti_2O_5 > Cu/K_2Ti_2O_5$. Actually, it is not surprising that $Ce/K_2Ti_2O_5$ exhibits the highest sulfation degree because it has been widely used as a sulfur trapping material.[32] These data further confirm that Cu is greater sulfur-resistant and has more potential to be used for NO_x abatement in the presence of sulfur.

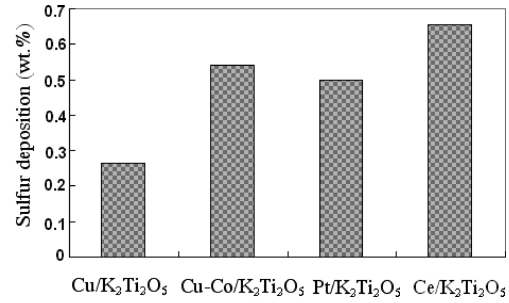

Figure 3. Sulfur deposition amounts on $Cu/K_2Ti_2O_5$, $Cu-Co/K_2Ti_2O_5$, $Pt/K_2Ti_2O_5$, and $Ce/K_2Ti_2O_5$.

3.2.2. Sulfur Species and Deactivation Mechanism. To overcome the sulfur poisoning effect, knowledge of the adsorbed sulfur species and the deactivation mechanism is very important. Therefore, the adsorbed sulfur species were investigated by using XRD, FTIR spectroscopy, and XPS. Figure S1 (Supporting Information) shows the XRD patterns of the freshly prepared and presulfated $K_2Ti_2O_5$. After 3 h of sulfation, the K_2SO_4 characteristic peaks located at 21.3°, 29.7°, 30.8°, and 43.4° were observed, and these peaks were strengthened after 10 h. Meanwhile, the $K_2Ti_2O_5$ structure gradually transformed into another potassium titanate with a lower K/Ti ratio ($K_2Ti_6O_{13}$). This phenomenon was more significant with the $Cu/K_2Ti_2O_5$ sample (Figure 4). Compared with the XRD patterns of the fresh $K_2Ti_6O_{13}$, it seems that $K_2Ti_2O_5$ support is transformed into $K_2Ti_6O_{13}$ after sulfation. Wang et al.[21,22,33] observed a $K_2Ti_2O_5-K_2Ti_6O_{13}$ structure switching phenomenon upon NO_2 adsorption and desorption, and they proposed the mechanism in reaction 1 and 2. The XRD analysis suggests that SO_2 might induce a similar structural change. The SO_2 molecules react with the K^+ ions located in the interlayers of $K_2Ti_2O_5$, and the shortage of K results in a regrouping of the remainder to other potassium titanates (mostly such as $K_2Ti_6O_{13}$), as shown in reaction 3.

$$3K_2Ti_2O_5 + 4NO_2 + O_2 \rightarrow K_2Ti_6O_{13} + 4KNO_3 \quad (1)$$

$$K_2Ti_6O_{13} + 4KNO_2 + 10H_2 \rightarrow 3K_2Ti_2O_5 + 2N_2 + 10H_2O \quad (2)$$

$$3K_2Ti_2O_5 + 2SO_2 + O_2 \rightarrow K_2Ti_6O_{13} + 2K_2SO_4 \quad (3)$$

The existence of SO_4^{2-} was further studied by FTIR spectroscopy and XPS. Figure 5 shows the FTIR spectra of the as-prepared and sulfated $Cu/K_2Ti_2O_5$ catalyst. After sulfation, the characteristic peaks of K_2SO_4 were observed at 619 and 1114 cm^{-1}. For the same sample, a S 2p binding energy of

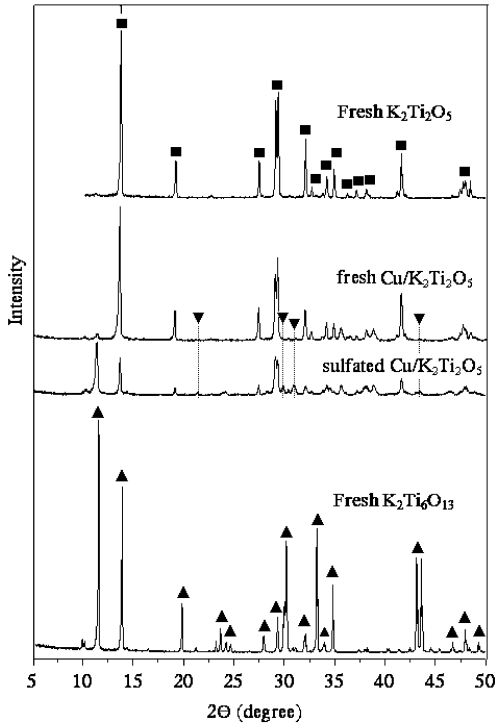

Figure 4. XRD patterns of fresh $K_2Ti_2O_5$, $K_2Ti_6O_{13}$, and sulfated $Cu/K_2Ti_2O_5$ catalysts. (▼) K_2SO_4 (JCPDS card 44-1413), (■) $K_2Ti_2O_5$ (JCPDS card 13-0448), (▲) $K_2Ti_6O_{13}$ (JCPDS card 40-0403).

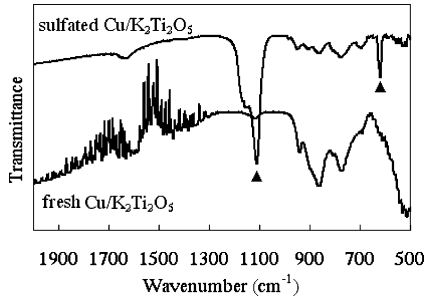

Figure 5. FTIR spectra of fresh and sulfated $Cu/K_2Ti_2O_5$ catalysts. (▲) K_2SO_4.

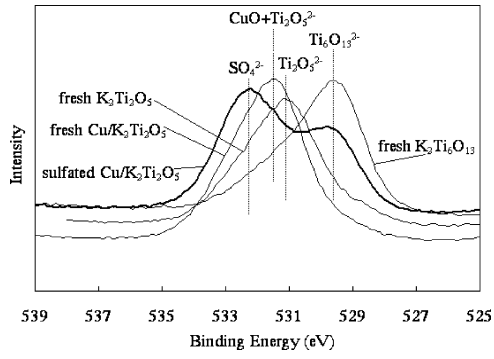

Figure 6. XPS spectra of O 1s for sulfated $Cu/K_2Ti_2O_5$, fresh $Cu/K_2Ti_2O_5$, fresh $K_2Ti_2O_5$, and fresh $K_2Ti_6O_{13}$.

169.5 eV, which was assigned to SO_4^{2-}, appeared in the sulfated sample, as compared to the fresh $Cu/K_2Ti_2O_5$ (Figure S2, Supporting Information).[2] Both FTIR and XPS analyses clearly indicate that the deposited sulfur was in the form of sulfate.

Figure 6 shows the XPS spectra of O 1s for the sulfated $Cu/K_2Ti_2O_5$, fresh $Cu/K_2Ti_2O_5$, fresh $K_2Ti_2O_5$, and fresh $K_2Ti_6O_{13}$ samples. For fresh $Cu/K_2Ti_2O_5$, $K_2Ti_2O_5$, and $K_2Ti_6O_{13}$, the O

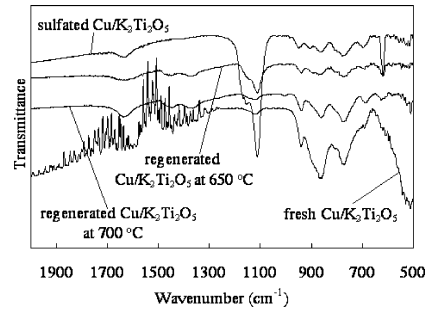

Figure 7. FTIR spectra of fresh $Cu/K_2Ti_2O_5$, sulfated $Cu/K_2Ti_2O_5$, and regenerated $Cu/K_2Ti_2O_5$ at 650 and 700 °C, respectively.

1s binding energies are located at around 531.4, 531.1, and 529.5 eV, respectively. The difference in O 1s between $K_2Ti_2O_5$ and $K_2Ti_6O_{13}$ is caused by their different atomic arrangements. After sulfation of $Cu/K_2Ti_2O_5$, two binding energy peaks of O 1s, 532.2 and 529.7 eV, were observed. The higher binding energy is attributed to SO_4^{2-}, and the lower binding energy is attributed to $K_2Ti_6O_{13}$. The XPS results provide additional direct evidence of the formation of potassium sulfate and the $K_2Ti_2O_5-K_2Ti_6O_{13}$ structure change. A similar result for the NO_x-adsorbed $K_2Ti_2O_5$ was also observed in our previous works.[21,22,33]

3.2.3. Regeneration of the Sulfated $Cu/K_2Ti_2O_5$. The stability of deposited sulfur species was evaluated by temperature-programmed reduction (TPR) with 3.5% H_2 from room temperature to 750 °C. Figure S3 (Supporting Information) shows the evolution of H_2S as a function of temperature. H_2S started to be released at 400 °C, with a peak temperature at 650 °C. Because $Cu/K_2Ti_2O_5$ is thermally stable up to 800 °C, the desulfurization process at high temperature will not cause any activity loss. The regeneration of sulfated $Cu/K_2Ti_2O_5$ at different temperatures (650 and 700 °C for 1 h) was also investigated by FTIR analyses (Figure 7). After regeneration at 650 °C, the characteristic peaks of sulfate (1114 and 619 cm^{-1}) were greatly weakened, indicating that the sulfated catalyst could be regenerated at 650 °C by allowing proper time. In contrast, at 700 °C, the catalyst was completely regenerated after 1 h.

3.2.4. Morphological Changes during SO_2 and NO_x Adsorptions. The morphological changes after SO_2 adsorption were investigated by SEM. Figure 8 shows SEM images of the fresh and sulfated $K_2Ti_2O_5$. Fresh $K_2Ti_2O_5$ showed flat, platelike particles with clean and smooth surfaces (Figure 8A); however, after being sulfated with SO_2 for a certain time, the structure was destroyed, and it gradually disintegrated into small particles (Figure 8B). A similar phenomenon was also observed with $Cu/K_2Ti_2O_5$. The surface of the $K_2Ti_2O_5$ support is very smooth, with well-dispersed nanosize CuO particles (Figure 9A). The SEM-EDX analyses in Figure S4 and S5 (Supporting Information) confirm that the supported particles are Cu, whereas after sulfation, the large $K_2Ti_2O_5$ particles are broken down into nanoparticles (Figure 9B). The formed particles have irregular shapes with an average size of around 500 nm. According to the XRD data (Figure 4), the nanoparticle compound is $K_2Ti_6O_{13}$.

The morphological changes caused by the coadsorption of NO_x and SO_2 were further investigated by pretreating $Cu/K_2Ti_2O_5$ with 200 ppm SO_2, 400 ppm NO, and 5% O_2 at 550 °C for 3 h, after which SEM analysis was performed. Figure 10A shows not only a nanoparticle-type compound ($K_2Ti_6O_{13}$) formed by SO_2 adsorption, but also a nanofiber-type compound. Figure 10B,C shows much clearer images of particle types 1 and 2, respectively. According to our previous report, the formation of particle type 2 is caused by NO_x adsorption.[21] Our

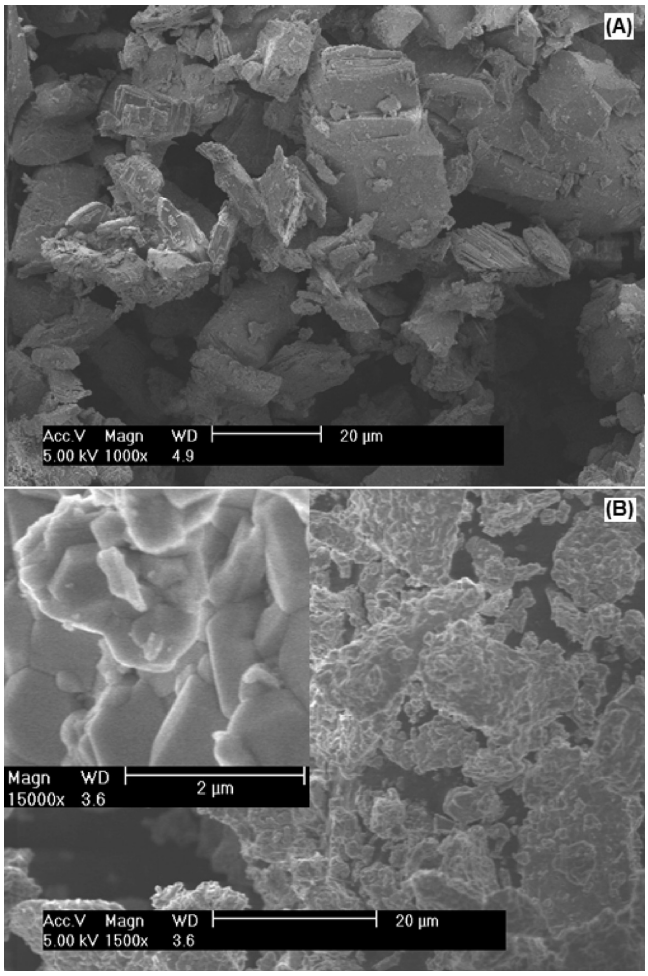

Figure 8. SEM images of (A) fresh and (B) sulfated $K_2Ti_2O_5$.

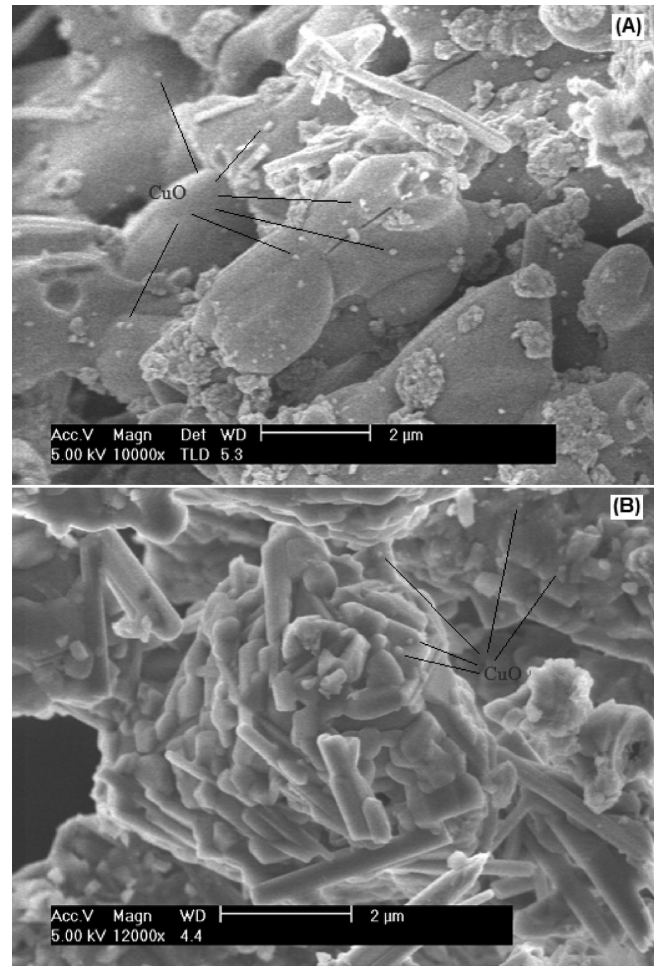

Figure 9. SEM images of (A) fresh and (B) sulfated $Cu/K_2Ti_2O_5$.

previous investigations have demonstrated that, with an increase in the NO_2 adsorption time, the structure of fresh $K_2Ti_2O_5$ gradually disintegrates into nanofibers.[33] These data suggest that, by adsorbing SO_2, $K_2Ti_2O_5$ tends to transform into the nanoparticle type $K_2Ti_6O_{13}$, whereas by adsorbing NO_x, $K_2Ti_2O_5$ tends to transform into the nanofiber type $K_2Ti_6O_{13}$. The coadsorption of NO_x and SO_2 is further supported by FTIR analysis (Figure S6, Supporting Information).[2,34] After pretreatment with both SO_2 and NO_x, both nitrate and sulfate species were detected.

Upon regeneration of the sulfated $Cu/K_2Ti_2O_5$ with 3.5% H_2 at different temperatures (650 and 700 °C) for 1 h, the formed nanoparticles recombined with each other and transformed back into larger particles, which were quite similar to the fresh $K_2Ti_2O_5$. Figure S7 (Supporting Information) shows the $Cu/K_2Ti_2O_5$ regenerated at 650 °C, with some small particles still remaining on the surface. In contrast, for the sample regenerated at 700 °C (Figure S8, Supporting Information), almost no small particles were found, and some interstices appeared, which might be due to the removal of previously formed K_2SO_4 crystalline. XRD analysis confirmed that the regenerated support was exactly the $K_2Ti_2O_5$ phase (not shown here).

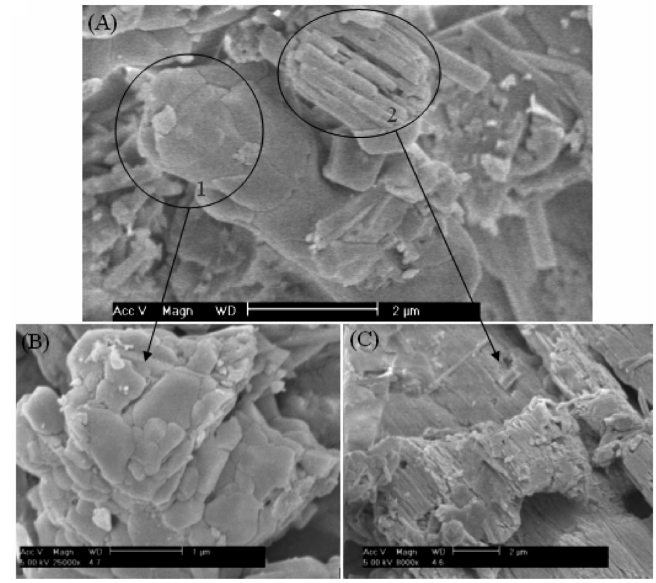

Figure 10. (A) SEM microstructure of $Cu/K_2Ti_2O_5$ pretreated with SO_2 and NO_x. Pretreatment conditions: 200 ppm SO_2, 400 ppm NO, 5% O_2, 200 mL/min, 550 °C, 3 h. (B,C) Enlarged images of indicated regions of part A.

4. Conclusions

The present work indicates that the thermal stability of the adsorbed SO_x species on the oxygen vacancies is much weaker than that of the sulfate salts (e.g., $BaSO_4$, K_2SO_4, etc.). The low-temperature sulfated $Cu/K_2Ti_2O_5$ can be easily regenerated by 3.5% H_2 at 550 °C. When the SO_2 concentration is less than 20 ppm, the sulfur poisoning effect is insignificant, and only a slight decrease in NO_x storage amount (within 15 min) is observed. At high temperature, $Cu/K_2Ti_2O_5$ accumulates the

least amount of sulfur, as compared to $Ce/K_2Ti_2O_5$, $Cu-Co/K_2Ti_2O_5$, and $Pt/K_2Ti_2O_5$. The deposited sulfur species is present in the form of sulfate, which is accompanied by a structure change between $K_2Ti_2O_5$ and $K_2Ti_6O_{13}$. SEM analysis indicates that, upon adsorbing SO_2, $K_2Ti_2O_5$ tends to transform into the nanoparticle type $K_2Ti_6O_{13}$, whereas upon adsorbing NO_x, $K_2Ti_2O_5$ tends to transform into the nanofiber type $K_2Ti_6O_{13}$. After regeneration, the formed $K_2Ti_6O_{13}$ nanoparticles recombine and transform back into $K_2Ti_2O_5$.

Supporting Information Available: XRD patterns of fresh $K_2Ti_2O_5$ and 3- and 10-h SO_2-adsorbed $K_2Ti_2O_5$, XPS spectra of S 2p for sulfated and fresh $Cu/K_2Ti_2O_5$, H_2S evolution of pre-sulfated $Cu/K_2Ti_2O_5$ as a function of temperature, SEM-EDX analyses of the $K_2Ti_2O_5$ support and the supported Cu of $Cu/K_2Ti_2O_5$ catalyst, FTIR analysis of $Cu/K_2Ti_2O_5$ pretreated with SO_2 and NO_x, and SEM microstructures of $Cu/K_2Ti_2O_5$ regenerated with 3.5% H_2 at 650 and 700 °C. This material is available free of charge via the Internet at http://pubs.acs.org.

Literature Cited

(1) Sedlmair, C.; Seshan, K.; Jentys, A.; Lercher, J. A. Studies on the Deactivation of NO_x Storage−Reduction Catalysts by Sulfur Dioxide. *Catal. Today* **2002**, *75*, 413.

(2) Engström, P.; Amberntsson, A.; Skoglundh, M.; Fridell, E.; Smedler, G. Sulphur Dioxide Interaction with NO_x Storage Catalysts. *Appl. Catal. B: Environ.* **1999**, *22*, L241.

(3) Elbouazzaoui, S.; Corbos, E. C.; Courtois, X.; Marecot, P.; Duprez, D. A Study of the Deactivation by Sulfur and Regeneration of a Model NSR $Pt/Ba/Al_2O_3$ Catalyst. *Appl. Catal. B: Environ.* **2005**, *61*, 236.

(4) Kim, J. G.; Lee, H. M.; Lee, M. J.; Lee, J. H.; Kim, J. G.; Jeon, J. Y.; Jeong, S. K.; Yoo, S. J.; Kim, S. S. Effect of Co and Rh Promoter on NO_x Storage and Reduction over $Pt/BaO/Al_2O_3$ Catalyst. *J. Ind. Eng. Chem.* **2008**, *14*, 841.

(5) Liu, Y.; Meng, M.; Li, X. G.; Guo, L. H.; Zha, Y. Q. NO_x Storage Behavior and Sulfur-Resisting Performance of the Third-Generation NSR Catalysts $Pt/K/TiO_2-ZrO_2$. *Chem. Eng. Res. Des.* **2008**, *86*, 932.

(6) Xiao, J.; Li, X.; Deng, S.; Wang, F.; Wang, L. NO_x Storage−Reduction over Combined Catalyst $Mn/Ba/Al_2O_3-Pt/Ba/Al_2O_3$. *Catal. Commun.* **2008**, *9*, 563.

(7) Casapu, M.; Grunwaldt, J. D.; Maciejewski, M.; Krumeich, F.; Baiker, A.; Wittrock, M.; Eckhoff, S. Comparative Study of Structural Properties and NO_x Storage−Reduction Behavior of $Pt/Ba/CeO_2$ and $Pt/Ba/Al_2O_3$. *Appl. Catal. B: Environ.* **2008**, *78*, 288.

(8) Piacentini, M.; Maciejewski, M.; Baiker, A. NO_x Storage−Reduction Behavior of $Pt-Ba/MO_2$ ($MO_2 = SiO_2, CeO_2, ZrO_2$) Catalysts. *Appl. Catal. B: Environ.* **2007**, *72*, 105.

(9) Epling, W. S.; Campbell, L. E.; Yezerets, A.; Currier, N. W.; Parks II, J. E. Overview of the Fundamental Reactions and Degradation Mechanisms of NO_x Storage/Reduction Catalysts. *Catal. Rev. Sci. Eng.* **2004**, *46*, 163.

(10) Takeuchi, M.; Matsumoto, S. NO_x Storage−Reduction Catalysts for Gasoline Engines. *Top. Catal.* **2004**, *28*, 151.

(11) Takahashi, N.; Suda, A.; Hachisuka, I.; Sugiura, M.; Sobukawa, H.; Shinjoh, H. Sulfur Durability of NO_x Storage and Reduction Catalyst with Supports of TiO_2, ZrO_2 and ZrO_2-TiO_2 Mixed Oxides. *Appl. Catal. B: Environ.* **2007**, *72*, 187.

(12) Rohr, F.; Peter, S. D.; Lox, E.; Kogel, M.; Sassi, A.; Juste, L.; Rigaudeau, C.; Belot, G.; Gelin, P.; Primet, M. On the Mechanism of Sulphur Poisoning and Regeneration of a Commercial Gasoline NO_x-Storage Catalyst. *Appl. Catal. B: Environ.* **2005**, *56*, 201.

(13) Limousy, L.; Mahzoul, H.; Brilhac, J. F.; Garin, F.; Maire, G. SO_2 Sorption on Fresh and Aged SO_x Traps. *Appl. Catal. B: Environ.* **2003**, *42*, 237.

(14) Limousy, L.; Mahzoul, H.; Brilhac, J. F.; Garin, F.; Maire, G.; Gilot, P. A Study of the Regeneration of Fresh and Aged SO_x Adsorbers under Reducing Conditions. *Appl. Catal. B: Environ.* **2003**, *43*, 169.

(15) Breen, J. P.; Marella, M.; Pistarino, C.; Ross, J. R. H. Sulfur-Tolerant NO_x Storage Traps: An Infrared and Thermodynamic Study of the Reactions of Alkali and Alkaline-Earth Metal Sulfates. *Catal. Lett.* **2002**, *80*, 123.

(16) Balcon, S.; Potvin, C.; Salin, L.; Tempère, J. F.; Djéga-Mariadassou, G. Influence of CO_2 on Storage and Release of NO_x on Barium-Containing Catalyst. *Catal. Lett.* **1999**, *60*, 39.

(17) Weast, R., Ed. *CRC Handbook of Chemistry and Physics*, 56th ed.; CRC Press: Boca Raton, FL, 1975−1976.

(18) Erkfeldt, S.; Larsson, M.; Hedblom, H.; Skoglundh, M. *Sulphur Poisoning and Regeneration of NO_x Trap Catalyst for Direct-Injected Gasoline Engines*; SAE Technical Paper Series 1999-01-3504; SAE International: Warrendale, PA, 1999.

(19) Takahashi, Y.; Takeda, Y.; Kondo, M.; Murata, N. *Development of NO_x Trap System for Commercial Vehicle-Basic Characteristics and Effects of Sulfur Poisoning*; SAE Technical Paper Series 2004-01-0580; SAE International: Warrendale, PA, 2004.

(20) AL-Harbi, M.; Epling, W. S. The Effects of Regeneration-Phase CO and/or H_2 Amount on the Performance of a NO_x Storage/Reduction Catalyst. *Appl. Catal. B: Environ.* **2009**, *89*, 315.

(21) Wang, Q.; Chung, J. S. NO_x Storage and Reduction over $Cu/K_2Ti_2O_5$ in a Wide Temperature Range: Activity, Characterization, and Mechanism. *Appl. Catal. A: Gen.* **2009**, *358*, 59.

(22) Wang, Q.; Sohn, J. H.; Chung, J. S. Thermally Stable $Pt/K_2Ti_2O_5$ as High-Temperature NO_x Storage and Reduction Catalyst. *Appl. Catal. B: Environ.* **2009**, *89*, 97.

(23) Andersson, S.; Wadsley, A. D. Five Co-ordinated Titanium in $K_2Ti_2O_5$. *Nature* **1960**, *187*, 499.

(24) Meng, X.; Wang, D.; Liu, J.; Lin, B.; Fu, Z. Effects of Titania Different Phases on the Microstructure and Properties of $K_2Ti_6O_{13}$ Nanowires. *Solid State Commun.* **2006**, *137*, 146.

(25) Liu, C.; He, M.; Lu, X.; Zhang, Q.; Xu, Z. Reaction and Crystallization Mechanism of Potassium Dititanate Fibers Synthesized by Low-Temperature Calcination. *Cryst. Growth Des.* **2005**, *5*, 1399.

(26) Luo, J. Y.; Meng, M.; Zha, Y. Q.; Xie, Y. N.; Hu, T. D.; Zhang, J.; Liu, T. A Comparative Study of $Pt/Ba/Al_2O_3$ and $Pt/Fe-Ba/Al_2O_3$ NSR Catalysts: New Insights into the Interaction of Pt−Ba and the Function of Fe. *Appl. Catal. B: Environ.* **2008**, *78*, 38.

(27) Zhao, Y.; Liu, Z.; Jia, Z. Elementary Sulfur Recovery by H_2-Regeneration of SO_2-Adsorbed CuO/Al_2O_3-Effect of Operation Parameters. *Chem. Eng. J.* **2007**, *134*, 11.

(28) Xie, G.; Liu, Z.; Zhu, Z.; Liu, Q.; Ge, J.; Huang, Z. Simultaneous Removal of SO_2 and NO_x from Flue Gas Using a CuO/Al_2O_3 Catalyst Sorbent: I. Deactivation of SCR Activity by SO_2 at Low Temperatures. *J. Catal.* **2004**, *224*, 36.

(29) Xie, G.; Liu, Z.; Zhu, Z.; Liu, Q.; Ge, J.; Huang, Z. Simultaneous Removal of SO_2 and NO_x from Flue Gas Using a CuO/Al_2O_3 Catalyst Sorbent: II. Promotion of SCR Activity by SO_2 at High Temperatures. *J. Catal.* **2004**, *224*, 42.

(30) Pietrogiacomi, D.; Magliano, A.; Sannino, D.; Campa, M. C.; Ciambelli, P.; Indovina, V. In Situ Sulphated CuO_x/ZrO_2 and CuO_x/Sulphated-ZrO_2 as Catalysts for the Reduction of NO_x with NH_3 in the Presence of Excess O_2. *Appl. Catal. B: Environ.* **2005**, *60*, 83.

(31) Xie, G.; Liu, Z.; Zhu, Z.; Liu, Q.; Ma, J. Reductive Regeneration of Sulfated CuO/Al_2O_3 Catalyst−Sorbent in Ammonia. *Appl. Catal. B: Environ.* **2003**, *45*, 213.

(32) Tikhomirov, K.; Krocher, O.; Elsener, M.; Widmer, M.; Wokaun, A. Manganese Based Materials for Diesel Exhaust SO_2 Traps. *Appl. Catal. B: Environ.* **2006**, *67*, 160.

(33) Wang, Q.; Guo, Z.; Chung, J. S. Molecular NO_2 Induced $K_2Ti_2O_5-K_2Ti_6O_{13}$ Structure Switching in the Dry Gas Phase: Lattice Potassium Reactivity. *Chem. Commun.* **2009**, *35*, 5284.

(34) Wang, Q.; Park, S. Y.; Choi, J. S.; Chung, J. S. $Co/K_xTi_2O_5$ Catalysts Prepared by Ion Exchange Method for NO Oxidation to NO_2. *Appl. Catal. B: Environ.* **2008**, *79*, 101.

Received for review April 23, 2010
Revised manuscript received May 30, 2010
Accepted June 24, 2010

IE1009525